

# Prototype of a frictionless linear motor with compliant bearings for precision engineering applications

Hai Nhan Le<sup>1,2</sup>, Huy Truong Nguyen<sup>1,2</sup>, Thuy Anh Le<sup>1,2</sup>, Minh Tuan Pham<sup>1,2,\*</sup>

## ABSTRACT

The paper presents the structural optimization and experimental evaluation of a novel linear motor for applications in precision engineering industry. The output linear motion from the motor is supposed to be highly accurate since it is supported by a couple of compliant bearings and a frictionless electromagnetic actuator. The 6-mm stroke of the proposed motor is determined by the largest displacement of compliant bearings in elastic region under the acting of more than 6-N axial force, i.e., both analytical and finite element methods (FEM) are applied before fabricating the motor prototype. By employing beam-type flexures, the design of compliant bearing is able to produce large elastic deformation while maintaining its stability during practical operation in high-frequency condition. In addition, the bearing design is optimized using the response surface methodology (RSM) through ANSYS, which is coupled with the previous static analysis by FEM, to achieve a compliant structure with even higher deformation capability in desired directions. The optimized bearings are then assembled with the voice coil actuator (VCA) to create a complete 1-DOF frictionless linear motor, this actuator is designed to fit the required maximum force for a pair of compliant mechanisms with the force/displacement relationship  $\sim 1$ . Several experimental evaluations are then carried out to verify the actual performance of the motor, e.g., highly linear transfer function and displacement error, under the input DC current 0-5A. The experimental results suggest that the proposed linear motor is able to produce precise translational motion with significant accuracy and high repeatability at micro-scale. Furthermore, the millimeter-scale stroke of the motor is large enough to integrate into variety of devices for precision engineering applications such as control valves, robotic components or even actuation in space, etc.

**Key words:** Linear motor, compliant bearing, compliant mechanism, optimization, response surface methodology

<sup>1</sup>Department of Machine Design, Faculty of Mechanical Engineering, Ho Chi Minh City University of Technology (HCMUT), 268 Ly Thuong Kiet Street, District 10, Ho Chi Minh City, Vietnam

<sup>2</sup>Vietnam National University Ho Chi Minh City, Linh Trung Ward, Thu Duc City, Ho Chi Minh City, Vietnam

## Correspondence

**Minh Tuan Pham**, Department of Machine Design, Faculty of Mechanical Engineering, Ho Chi Minh City University of Technology (HCMUT), 268 Ly Thuong Kiet Street, District 10, Ho Chi Minh City, Vietnam

Vietnam National University Ho Chi Minh City, Linh Trung Ward, Thu Duc City, Ho Chi Minh City, Vietnam

Email: pminhtuan@hcmut.edu.vn

## History

- Received: 27-02-2024
- Revised: 10-8-2024
- Accepted: 22-10-2024
- Published Online: 31-12-2024

## DOI :

<https://doi.org/10.32508/stdjet.v7i3.1344>



## INTRODUCTION

For every precise positioning system, two key factors that reduce the precision of desired motions are friction and inertia. Popular actuators and mechanisms, such as pneumatic systems, servo motors with screw shaft, slider-crank linkages, have unavoidable inertia, especially when working in high-speed or in microscale/ nanoscale range. Meanwhile, the friction between mechanical components cannot be estimated accurately after a period of used time due to various reasons, such as lubrication, wear of material caused by dry friction and many other unpredictable errors in manufacturing and assembly processes. To overcome such limitations, compliant mechanisms can be considered as a potential solution for applications with relative-small working range, high precision, good repeatability, lubrication- and maintenance-free.

In this work, the elastic deformation of a thin beam-type compliant mechanism is employed to create desired output motions of compliant bearings. As a result, the compliant bearings can eliminate the iner-

tia by spring force and produce precise displacement based on Hooke's law. In addition, by combining a pair of compliant bearings with a voice coil actuator (VCA), a novel linear motor actuated by electromagnetic force can be archived to perform frictionless and precise motion.

Referring to previous literatures, the compliant mechanism can be designed based on the combination between rigid and deformable beam elements<sup>1-3</sup>. To improve the maximum deformation of the bearings while the original structure<sup>4,5</sup> is remained, the dimensions of each beam are set as design variables for static structural analysis<sup>6,7</sup> in ANSYS. By varying the values of these variables according to the constraints for beam dimensions, the output displacement and von Mises stress data can be collected to build the response surfaces<sup>8,9</sup>. From these response surfaces, the optimized design that can produce large elastic deformation along the desired direction and has large stiffness in non-actuating directions can be achieved. The mentioned literatures presented a variety of synthesis

**Cite this article :** Le H N, Nguyen H T, Le T A, Pham M T. **Prototype of a frictionless linear motor with compliant bearings for precision engineering applications.** *Sci. Tech. Dev. J. – Engineering and Technology* 2024; 7(3):2380-2392.

# Copyright

© VNUHCM Press. This is an open-access article distributed under the terms of the Creative Commons Attribution 4.0 International license.



and optimization methods for compliant mechanism, but most previous work only provided some individual compliant mechanism designs as case studies for demonstrating the methods and have not considered their industrial applications. In this work, a novel design of compliant bearing is optimized based on the existing methods. Its design is specific for a linear motor, which is developed for precise motion systems. From the optimized compliant bearing, a voice coil module<sup>10</sup> is then designed to fit the dimensions and provide the required force for the deformation of compliant bearings. To simplify the control system and reduce the burden of signal linearization like previous actuators<sup>11,12</sup>, the testing module is aimed to have an open-loop control system with a linear transfer function that is developed based on the relationships between applied DC voltage, electromagnetic force and translational displacement. Typically, a VCA needs a translational joint to produce the desired linear motion. In this work, the compliant bearings and voice coil module are designed to fit each other to create a unique linear motor with simple structure, but is capable of producing high accurate linear motion by exploiting the frictionless property of compliant mechanism. A prototype of the motor is then built and experimentally tested to demonstrate its effectiveness.

The remaining of the paper is organized as follow: design of the linear motor, optimization process, experiment setup, optimization result, experiment result and conclusion.

## RESEARCH METHOD

### Design of the Linear Motor

The linear motor consists of two main modules: a pair of compliant bearings and a voice coil actuator (illustrated in Figure 1) with the targeted boundary dimensions being limited to 100mm x 100mm x 180mm to fit popular precise motion systems. The rotor shaft of the VCA, which is assembled with the central flanges (moving bodies) of two bearings, will generate electromagnetic force when a DC voltage value is applied and will make the compliant mechanisms deform. The stator of the VCA is mounted to the fixed bodies of compliant bearings as shown in Figure 2. The actuated position of the rotor shaft is located at the midpoint between bearing centers so that each compliant mechanism can be acted by equal force and producing identical displacement.

Based on previous works<sup>4</sup>, the initial model of the compliant bearing is designed and calculated by applying the serial-parallel relationships between beam

elements (Figure 2). In particular, the bearing consists of four symmetrical legs about its center. Each leg is constructed by five beam-type flexures connected serially. In this design, all of the beams have the same thickness  $b$  and width  $h$ , only the lengths  $L$  of them are changed to well fulfill the given design space. For the bearing material, aluminum alloy 6061 is selected due to its popularity in the compliant mechanism. The detailed mechanical properties of this material are given in Table 1.

Based on the Hooke's law in equation (1), to control the displacement  $x$  of compliant bearings, the total stiffness  $k$  along  $z$  axis of beam elements will be determined by using 6x6 stiffness matrix of a typical fixed-end beam (2) for each beam element above and then synthesizing these matrices together following relationships in Figure 3.

$$F = k \cdot x \quad (1)$$

Where:  $F$ : Applied force (elastic force) (N)

$k$ : Stiffness of element (Nm)

$x$ : Displacement of element (m)

$$K_{beam} = \begin{bmatrix} \frac{AE}{L} & 0 & 0 & 0 & 0 & 0 \\ 0 & \frac{12EI_z}{L^3} & 0 & 0 & 0 & -\frac{6EI_z}{L^2} \\ 0 & 0 & \frac{12EI_y}{L^3} & 0 & \frac{EI_y}{L^2} & 0 \\ 0 & 0 & 0 & \frac{GJ}{L} & 0 & 0 \\ 0 & 0 & \frac{6EI_y}{L^2} & 0 & \frac{4EI_y}{L} & 0 \\ 0 & -\frac{6EI_z}{L^2} & 0 & 0 & 0 & \frac{4EI_z}{L} \end{bmatrix} \quad (2)$$

Where:  $E$ : Young's modulus (MPa)

$G$ : Shear modulus (MPa)

$A$ : Cross-sectional area (m<sup>2</sup>)

$I_y$ : Inertia moment about  $y$  axis (m<sup>4</sup>)

$I_z$ : Inertia moment about  $z$  axis (m<sup>4</sup>)

$J$ : Torsion constant (m<sup>4</sup>)

To verify the calculated result, static structural analysis is also performed in Ansys software and the final result of maximum displacements for two methods is shown in Table 2.

From the required force to archive the maximum displacement of 2 compliant bearings and the boundary dimensions of the motor, a moving-coil VCA was designed with two components: stator and rotor (Figure 4). The strongest output force that this VCA can generate is estimated by the Lorentz force formula in equation (3) with the maximum voltage source 12V and the working current cannot exceed 10A.

$$F = i_{coil} l_{pass} B_{gap} \quad (3)$$

$F$ : Electromagnetic force (N)

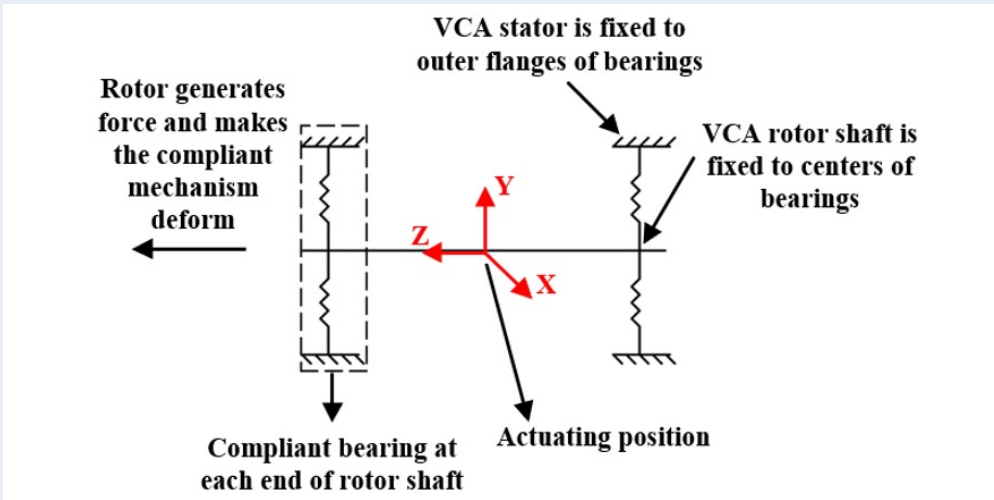


Figure 1: The kinematic diagram of linear motor.

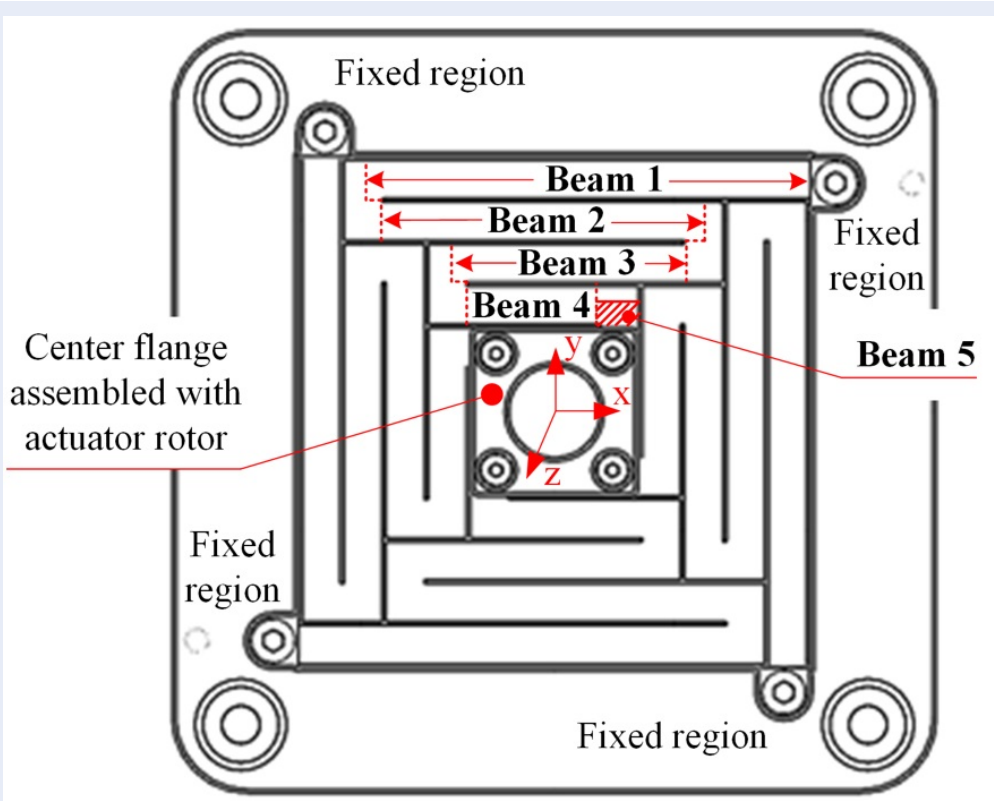
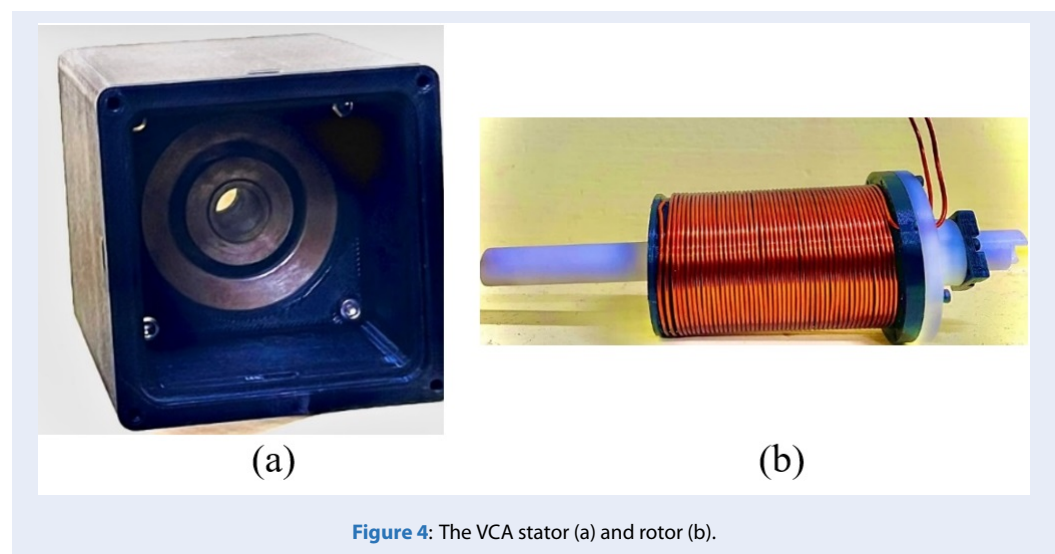
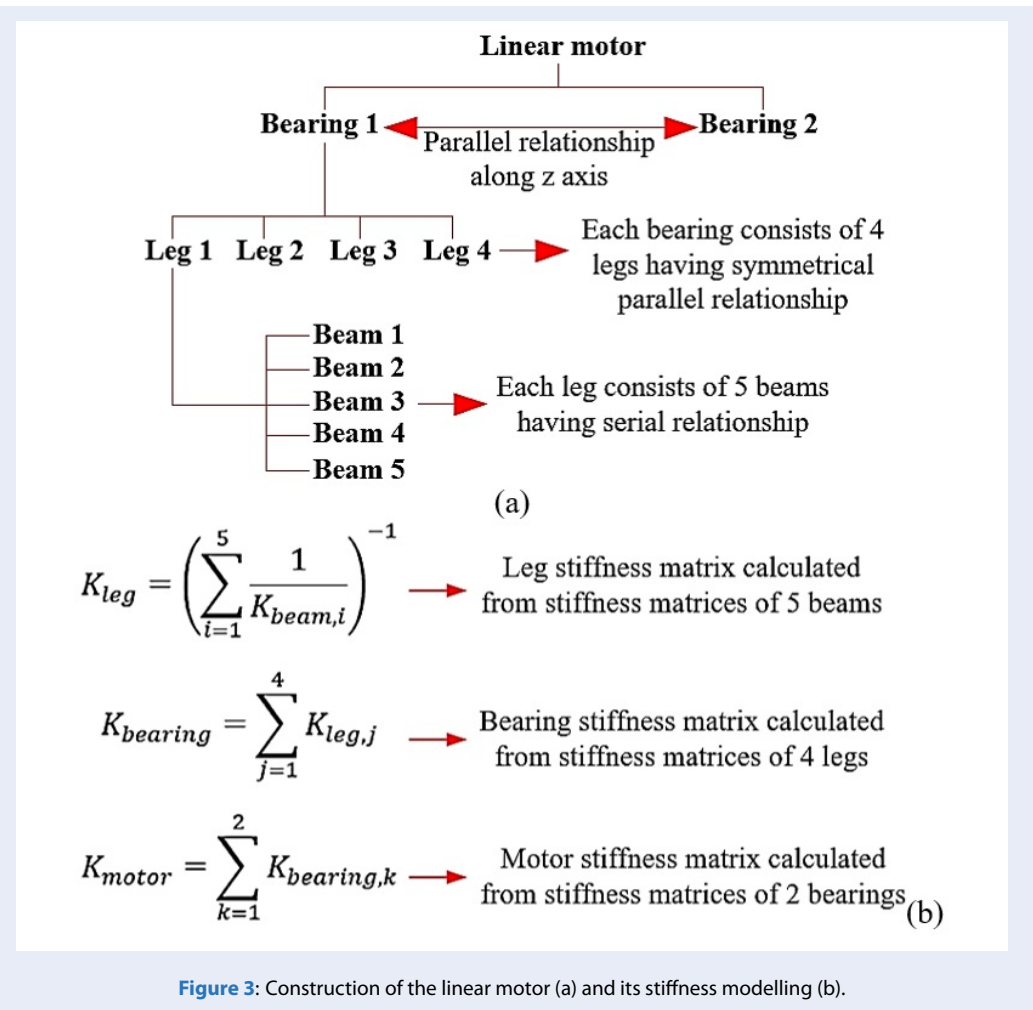


Figure 2: Original design for one leg of the compliant bearing.



**Table 1: Mechanical properties of aluminum alloy 6061**

Young's modulus	$E = 69 \times 10^9 \text{ N/m}^2$
Density	$D = 2700 \text{ kg/m}^3$
Poisson coefficient	$= 0.33$
Shear modulus	$G = 259 \times 10^8 \text{ kg/m}^3$
Yield strength	$YS = 276 \text{ MPa}$

**Table 2: Result of the initial motor with 2 compliant bearings**

Value	Maximum displacement -Stroke (mm)	Maximum required force (N)
Method		
Analytical method (Stiffness matrix)	6.2829	6.3785
Finite element method (Ansys simulation)	6.5699	6.3785
Error between 2 methods (%)	4.57	

$i_{coil}$ : Current through the rotor coil (A)

$l_{pass}$ : Length of the wire which flux lines pass (m)

$B_{gap}$ : Magnetic flux density (T)

While  $i_{coil}$  and  $l_{pass}$  can be determined from the number of wiring turns, the magnetic flux density of the VCA is calculated by both analytical method via equivalent closed magnetic circuit model and finite element method with magnetostatic simulation<sup>5</sup>. It is noted that the stator consists of the permanent magnet and a cover while the rotor is a coil as shown in Figure 4. From the calculation, the voice coil actuator can have maximum 3.2N linear force. This value will not satisfy the maximum force from Table 2 with nearly 6.4N. Therefore, an optimization is conducted to not only reduce the required force but also increase the maximum displacement.

### Structural Optimization

The aim of this optimization is to improve the maximum elastic displacement of the compliant bearings while decreasing the required force from 6.4N to 3.2N or lower. This section demonstrates the general model of optimization in ANSYS with a defined objective, constrains and then analyses the result data to determine the most effective structure for the compliant bearing prototype.

As the compliant bearing is constructed by 4-legged configuration, the structural optimization is conducted for one leg only. For each beam element, there are three dimensions that can be set as design variables for the optimization: Thickness  $b_i$ , width  $h_i$  and

length  $L_i$  of the beam  $i$  as shown in Figure 5a where  $i = 1, 2, 3, 4$ . From the formula of stiffness of a cantilever beam under bending (illustrated in Figure 5b) written in equation (4), it is obvious that the minimum thickness will provide the lowest stiffness, which also means the beam can perform a high bending flexibility about this direction effectively. Due to the complexity of using an ultra-thin metal plate for the accurate fabrication and assembly, the beam thicknesses in this work are kept as constant of 0.5mm to create the high flexibility of the compliant bearing and ensure its stable structure during the manufacturing and assembly processes.

$$k_{cantilever} = 3EI/l^3 = Ebh^3/4l^3 \quad (4)$$

Take advantage of the symmetrical design of the compliant bearing, seven dimensions of a leg are analysed as input variables as illustrated in Figure 6a. By this way, instead of setting ten variables for the lengths and widths of 5 beams, the number of design variables is minimized to 7 variables.

After defining the input variables for constraining, the output variables for the objective of optimization are also considered. There will be two parameters that are set as target variables: the center displacement (VCA rotor shaft position) of the compliant mechanism under the acting of 1N force (also known as the linear compliance of the bearing under an actuating force from the VCA) and the maximum von Mises stress in the bearing structure.

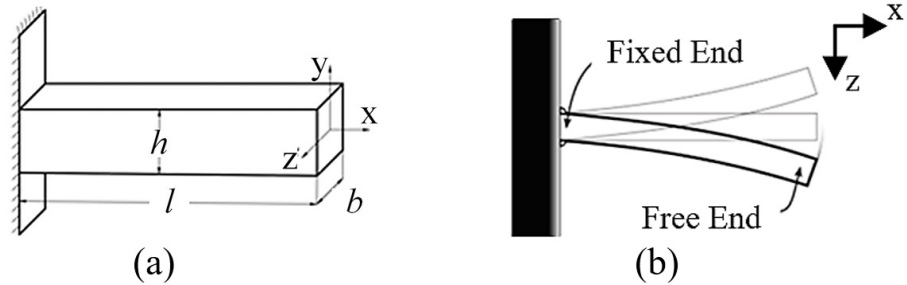


**Figure 5:** Design variables of each beam (a), bending cantilever beam model (b).

The objective of this optimization is to maximize the displacement of the compliant bearing under desired actuating force while its original structure is remained, and the von Mises stress is constrained to be lower than the yield strength of material as shown in Table 1.

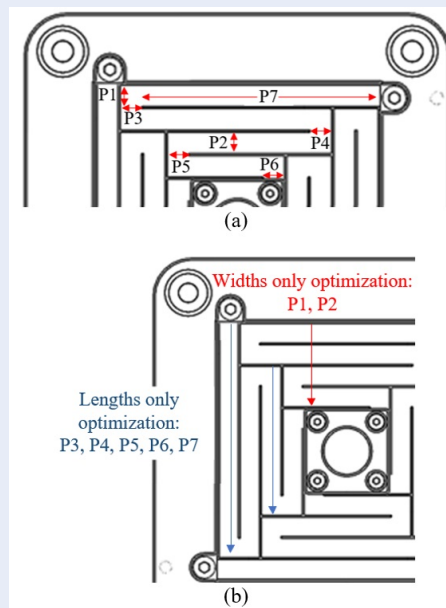


**Figure 6:** Optimization variables (a) Considered variables for each optimization case (b).

The result for displacement and von Mises stress variables with initial beam dimensions in Figure 2 will be calculated first in ANSYS and connected to 3 single-objective optimization (Pareto optimality) setups with different constraining cases, i.e., the input variables will change beam widths only, the input variables will change beam lengths only, the input variables will change both beam widths and lengths

(Figure 6b). The constraints for input variables will be defined based on the boundary dimensions of the motor model to avoid the penetration between beam elements. Each optimization setup will provide an output displacement - stress data and this result will be used to build response surfaces. By using the genetic algorithm (GA) with defined constraints and a single objective to maximize the output displacement along Z axis, the optimized dimensions of beam elements can be determined from ANSYS software.

There is also another method to archive the optimized dimensions, which is identifying the sweet spot of response surfaces by analysing the data from static structural analysis. Because the target is to maximize the displacement and minimize the stress, the ratio  $t$  between these two parameters can be determined for each dimensions combination in the result data following equation (5).

$$t = c_j / \sigma_{\max_j} \quad (5)$$

$t$ : Ratio between max displacement and max stress

$C_j$ : Maximum displacement under 1N force (mm)

$\sigma_{\max_j}$ : Maximum von Mises stress (MPa)

The combination with highest  $t$  will be the best result for optimization due to both high displacement and low stress. In reverse, the model with highest  $t$  or sweet spots of response surfaces is not always the finest design to build the prototype. Too low compliance can cause unstable motion when applying and dependent displacements along remaining DOFs. Thus, beside considering the sweet spots, the points which locate close to these spots must also need to be noticed.

## RESULTS

### Optimization result

From the optimization process, response surface results for 3 cases with the most influential design variables can be obtained and presented in Figures 7 and 8



and 9. Overall, 3 cases have quite similar optimized results for the new dimensions of beam elements and the best combination of each case is shown in Table 3. By using this data, each combination will be calculated by the stiffness matrix method from equation (2) and also performed in simulation again to determine which is the best one for building the prototype of the linear motor later.

By using above optimized dimensions, the new compliant bearing with ununiform beam elements is re-design in Figure 10 and analysed by finite element method in Figure 11.

The new model shown better deforming distribution especially for beams 1 and 3. The maximum displacement for the optimized motor is shown in Table 4. The motor stroke is determined by the ratio between the yield strength of aluminum and maximum von Mises stress from Figure 11b, this ratio is then multiplied with the highest displacement in Figure 11a.

By comparing results from Tables 2 and 4, it is seen that the optimized design has its deforming capability improved nearly 55%. Meanwhile, the maximum required force of the optimized design also fits to the output force generated by the proposed VCA module.

## Experimental setup

The experiment is conducted to study the linear transfer function with discrete input DC signal and has a preliminary investigation on the operating tolerance of the motor prototype.

To verify the actual performance of the optimized design, a linear motor prototype (Figure 12a) was built and an experimental setup was conducted to measure its translational displacement corresponding to a DC current value (Figure 12b). In this experiment, the motor prototype is clamped by a fixture. The output shaft then contacts directly with the dial indicator head to measure its translational displacement along the desired DOF. The dial indicator and fixture are both fixed to the ground to avoid external disturbances from the environment. The resolution for devices will be as follows: 0.2A for the DC power supply and 0.01mm for the dial indicator. The maximum current that the power supply can archive is 5A.

The measurement was carried out at room temperature of 20-25°C and repeated 10 measured times, the DC current increases from 1 to 5A with 0.2A interval. As a result, there are 25 data points for each measuring time.

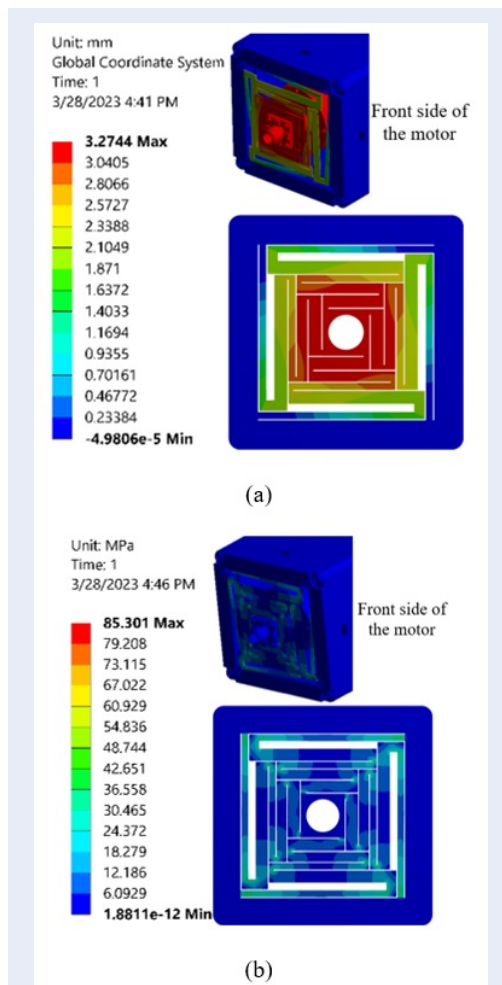


**Figure 11:** Simulation of the motor with two bearings for displacement (a) and von Mises stress (b) acted by 1N force.

## Actual Performance of the Frictionless Linear Motor

Based on the experimental result, the average curve demonstrates the highly linear relationship between input current and output displacement can be archived as shown in Figure 13. The maximum deviation between the average curve and measuring values is 19μm, while the highest deviation between measuring times is nearly 45μm. These micro-level differences can be explained by the limited resolution of 10μm and 0.2A from the dial indicator and DC power supply respectively. The experimental stroke has come up to 0.45mm at 4A input current due to the limitation of the DC power supply. With more advanced devices, the linear motor is supposed to achieve better performance in terms of resolution, accuracy, stroke and a linear characteristic. Overall,

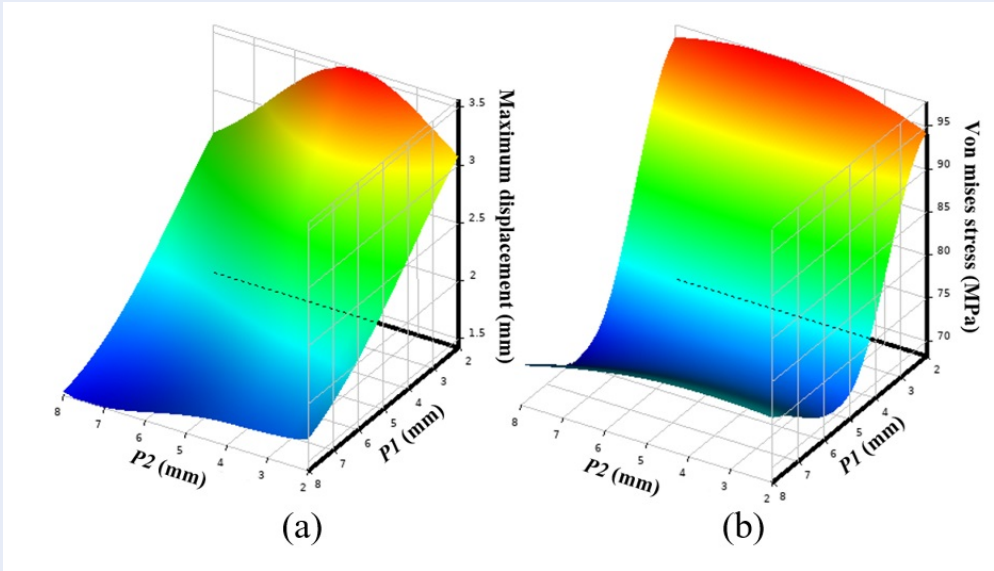


**Figure 7:** Response surface of displacement (a) and maximum von Mises stress (b) in beam widths only optimization.

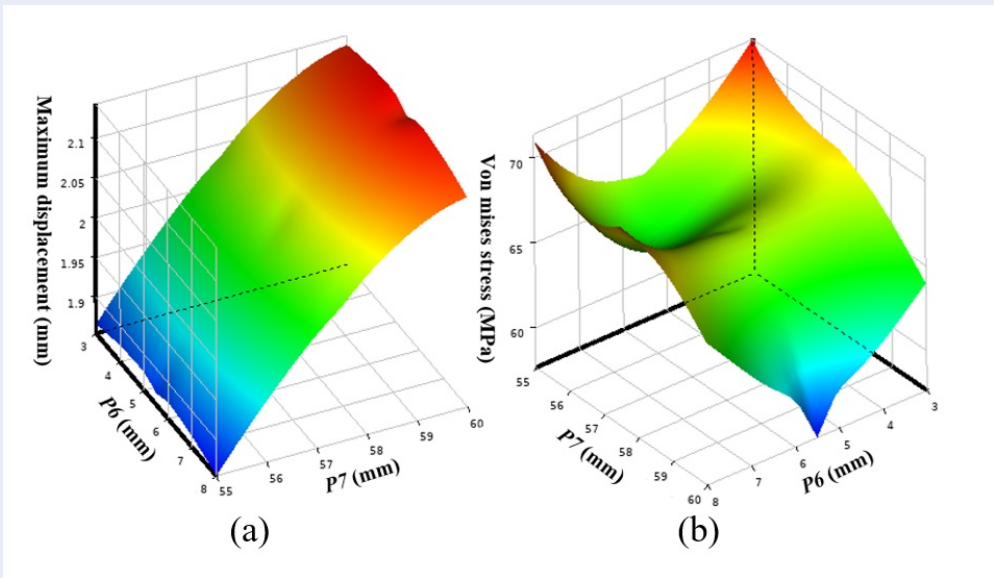


**Figure 8:** Response surface of displacement (a) and maximum von Mises stress (b) in beam lengths only optimization.

**Table 3:** Finest combinations of each optimization cases

Case	P1 (mm)	P2 (mm)	P3 (mm)	P4 (mm)	P5 (mm)	P6 (mm)	P7 (mm)
Width only	3	4	-	-	-	-	-
Length only	-	-	3	4	8	3	55
Width and length	3	4.5	3	4.5	4.5	5	58



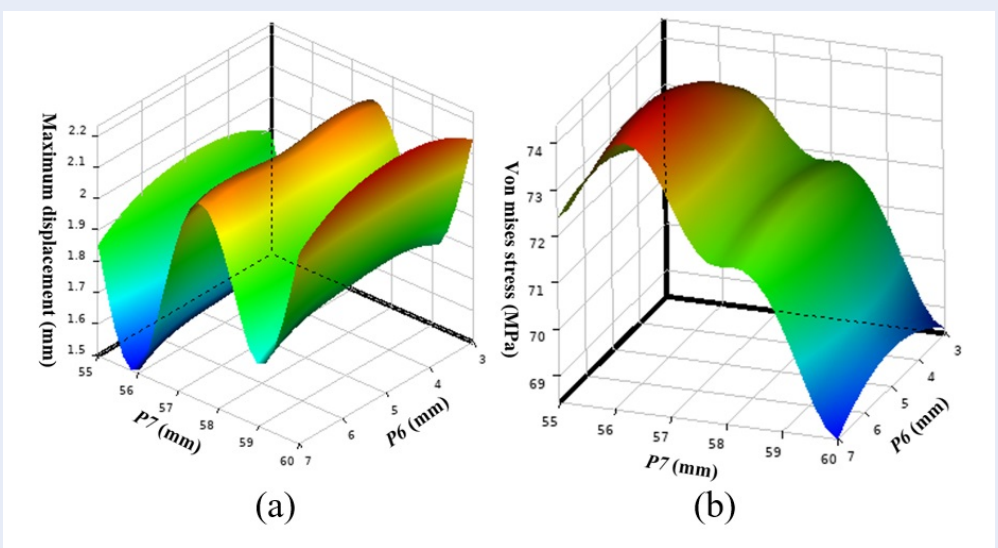


Figure 9: Response surface of displacement (a) and von Mises stress (b) in both beam widths and lengths optimization.

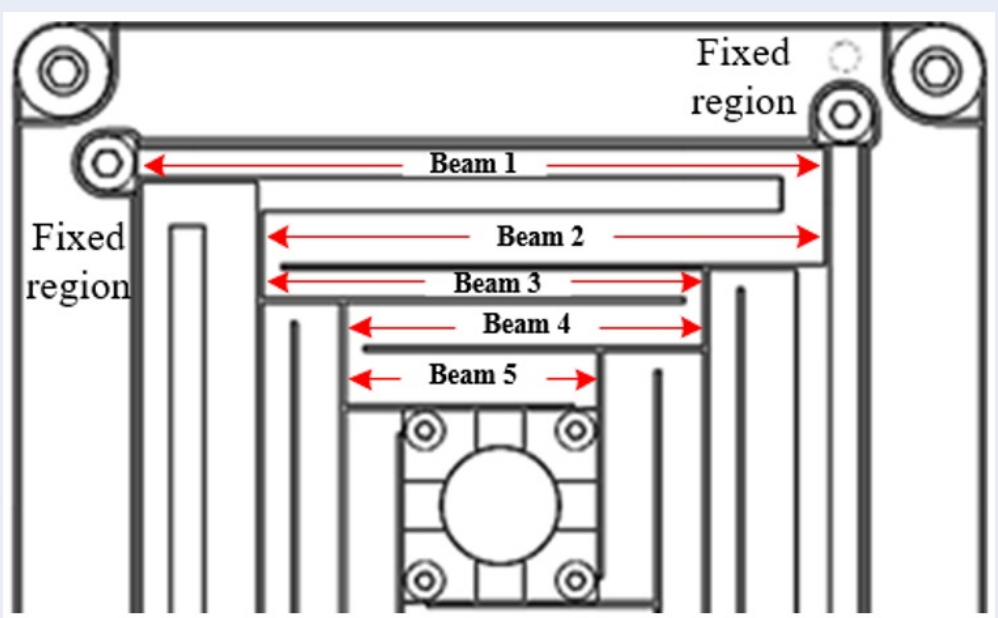
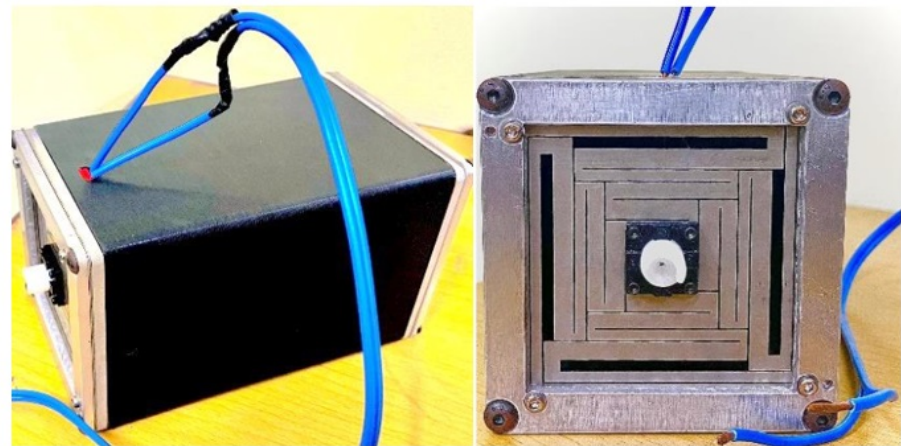


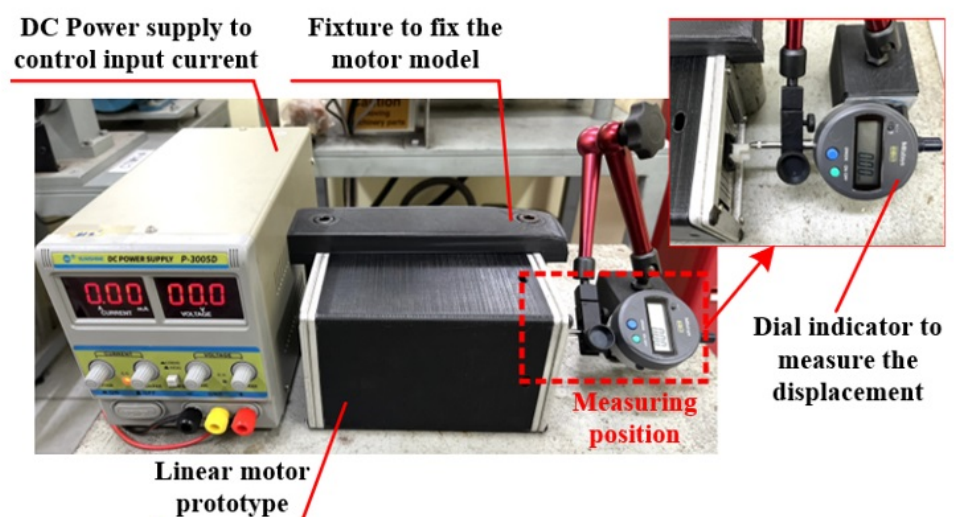
Figure 10: The optimized model of compliant bearing.

Table 4: Result of optimized motor with 2 compliant bearings

value	Maximum displacement -Stroke (mm)	Maximum required force (N)
Method		
Analytical method (Stiffness matrix)	10.2152	3.0757
Finite element method (Ansys simulation)	10.1694	3.0757



(a)



(b)

**Figure 12:** Linear motor prototype (a) and experimental setup for displacement measurement (b).

based on the experimental result, this motor model can guarantee the workspace up to more than 10mm (simulation result from Table 4). The experiments were repeated 25 times with 10 measured points each time. The measured results were then analyzed and the achieved result showed that the motor is able to perform a positioning tolerance of  $\pm 22.5$  micrometers.

## DISCUSSION

From the average curve of experimental result, the linear function in equation (6) demonstrating the relationship between the output displacement  $C$  (mm) and the input current  $i_{coil}$  (A) can be determined by linearization. This can be also used as the transfer

function for the open-loop control system of the linear motor.

$$C = 0.117 \times i_{coil} \quad (6)$$

It is noted that for the measurement in the electrical current range from 0A to 1A, the measured value can be unclear due to the small displacement and the initial reaction force by the dial indicator. Therefore, the measurement is conducted from 1A to 5A.

## CONCLUSION

The linear motor presented in this paper has shown the capability to work in micro-scale tolerance while still ensuring high repeatability as demonstrated by the experimental results. With the maximum stroke of more than 10 mm together with the linear char-

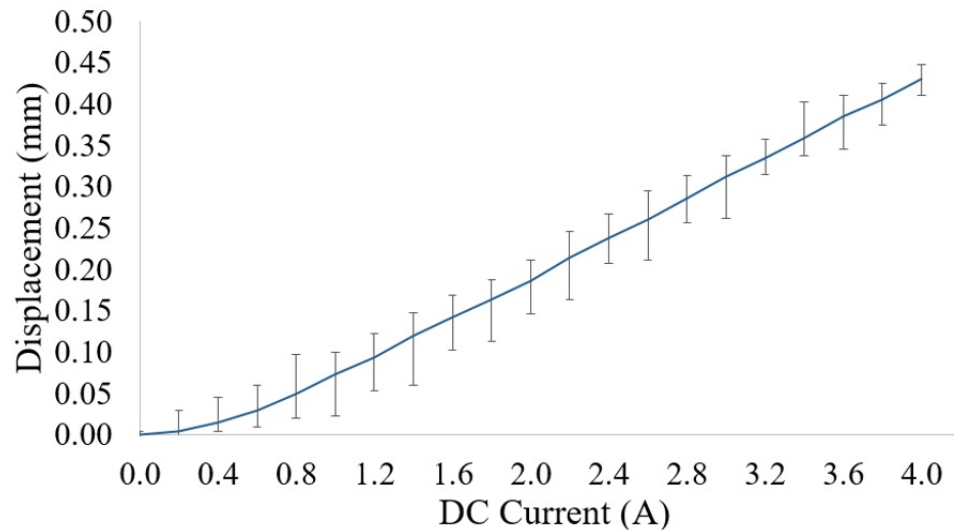


**Figure 13:** The average current-displacement curve with error bars for measured points

acteristic for open-loop control system, this type of motor will be a potential solution for high-precision industrial applications such as actuating systems of compact robotic modules, pick and place units of production lines, control valves in pneumatic systems, or even actuating apparatuses for aerospace engineering due to the maintenance-free characteristic, etc.

For the future, it is necessary to conduct the experiment in this paper again by devices with more accurate resolution and continuous input DC current; so that the tolerance of the motor can be identified precisely and the dynamic operation in a frequency range can be studied. Furthermore, the effect of temperature and errors caused by fabrication and assembly processes will be also considered to investigate.

## ACKNOWLEDGMENT

This research is funded by Ho Chi Minh City University of Technology – VNU-HCM, under grant number To-CK-2023-03.

## COMPETING INTEREST

The authors declare that they have no competing interests.

## AUTHORS CONTRIBUTION

H. N. Le: Conceptualization, Prototype Development, Investigation and Manuscript Preparation. H. T. Nguyen: Investigation, Validation and Manuscript Editing. T. A. Le: Design Optimization and Validation. M. T. Pham: Methodology, Funding Acquisition,

Resources, Validation and Manuscript Editing.

## REFERENCES

1. Teo TJ, Yang G, Chen I-M. A flexure-based electromagnetic nanopositioning actuator with predictable and re-configurable open-loop positioning resolution. *Precision Engineering*. 2015;40:249–60;.
2. Zhu J, Hao G. Modelling of a general lumped-compliance beam for compliant mechanisms. *International Journal of Mechanical Sciences*. 2023;108779;.
3. Arumugam P, Kumar A. Design methods for compliant mechanisms used in new age industries: A review. *Istrazivanja i projektovanja za privredu*. 2016;14(2):223-32; Available from: <http://dx.doi.org/10.5937/jaes14-8229>.
4. Hai NL, Phuc KN, Minh TP. Design and simulation of a linear-motion compliant mechanism. *The 2023 International Symposium on Advanced Engineering*. 2023; Available from: [https://dost.hochiminhcity.gov.vn/documents/1661/K%E1%BB%B7\\_y%E1%BA%BFu\\_H%E1%BB%99i\\_ngh%E1%BB%8B\\_ISAE2023\\_Edited\\_Final.pdf](https://dost.hochiminhcity.gov.vn/documents/1661/K%E1%BB%B7_y%E1%BA%BFu_H%E1%BB%99i_ngh%E1%BB%8B_ISAE2023_Edited_Final.pdf).
5. Hai NL, Phuc KN, Minh TP. Design and simulation of a low-cost frictionless linear motor. *Advances in Science and Technology*. 2024;136:17-22; Available from: <https://doi.org/10.4028/p-TRn4PH>.
6. Sivadas S. Static structural analysis of different materials for connecting rod. *International Journal for Research in Applied Science and Engineering Technology*. 2021;9(12):1083–9;.
7. Albanesi AE, Pucheta MA, Fachinotti VD. A new method to design compliant mechanisms based on the inverse beam finite element model. *Mechanism and Machine Theory*. 2013;65:14–28; Available from: <https://doi.org/10.1016/j.mechmachtheory.2013.02.009>.
8. Yang R, Li W, Liu Y. A novel response surface method for structural reliability. *AIP Advances*. 2022;12(1);.
9. Zhou L, Wang L, Chen L, Ou J. Structural finite element model updating by using response surfaces and radial basis functions. *Advances in Structural Engineering*. 2016;19(9):1446–62;.

10. Baronti F, Lazzeri A, Lenzi F, Roncella R, Saletti R, Saponara S. Voice coil actuators: From model and simulation to Automotive Application. 2009 35th Annual Conference of IEEE Industrial Electronics. 2009;.
11. Si-Lu Chen, Tat Joo Teo, Guilin Yang. Control of an 2-DOF electromagnetic actuator for high precision and high-throughput pick-and-place tasks. 2013 IEEE/ASME International Conference on Advanced Intelligent Mechatronics. 2013;.
12. Wang X, Chen W, Wang J, Song S. Closed-loop electromagnetic actuation system for magnetic capsule robot in a large scale. 2022 IEEE International Conference on Real-time Computing and Robotics (RCAR). 2022;.

# Mô hình động cơ tịnh tiến không ma sát với gối đỡ đàn hồi cho các ứng dụng trong cơ khí chính xác

Lê Hải Nhân<sup>1,2</sup>, Nguyễn Huy Trường<sup>1,2</sup>, Lê Thúy Anh<sup>1,2</sup>, Phạm Minh Tuấn<sup>1,2,\*</sup>

<sup>1</sup>Bộ Môn Thiết Kế Máy, Khoa Cơ Khí, Trường Đại học Bách khoa Tp. HCM (HCMUT), 268 Lý Thường Kiệt, Quận 10, Thành phố Hồ Chí Minh, Việt Nam

<sup>2</sup>Đại học Quốc gia Thành phố Hồ Chí Minh, Phường Linh Trung, Thành phố Thủ Đức, Thành phố Hồ Chí Minh, Việt Nam

## Liên hệ

**Phạm Minh Tuấn**, Bộ Môn Thiết Kế Máy, Khoa Cơ Khí, Trường Đại học Bách khoa Tp. HCM (HCMUT), 268 Lý Thường Kiệt, Quận 10, Thành phố Hồ Chí Minh, Việt Nam

Đại học Quốc gia Thành phố Hồ Chí Minh, Phường Linh Trung, Thành phố Thủ Đức, Thành phố Hồ Chí Minh, Việt Nam

Email: pminhtuan@hcmut.edu.vn

## Lịch sử

- Ngày nhận: 27-2-2024
- Ngày sửa đổi: 10-8-2024
- Ngày chấp nhận: 22-10-2024
- Ngày đăng: 31-12-2024

DOI : <https://doi.org/10.32508/stdjet.v7i3.1344>



## Bản quyền

© ĐHQG Tp.HCM. Đây là bài báo công bố mở được phát hành theo các điều khoản của the Creative Commons Attribution 4.0 International license.



## TÓM TẮT

Bài báo này trình bày việc tối ưu hóa kết cấu và đánh giá thực nghiệm một loại động cơ tuyến tính mới phục vụ cho các ứng dụng trong ngành công nghiệp cơ khí chính xác. Chuyển động tịnh tiến từ động cơ có độ chính xác cao vì trục động cơ được lắp trên một cặp gối đỡ đàn hồi và vận hành bằng một cơ cấu chấp hành điện từ không ma sát. Hành trình tối đa 6 mm của động cơ được xác định thông qua độ dịch chuyển lớn nhất của gối đỡ trong vùng đàn hồi dưới tác dụng của lực dọc trục hơn 6 N (cả phương pháp giải tích và phương pháp phần tử hữu hạn (FEM) đều được áp dụng cho việc tính toán trước khi chế tạo mô hình động cơ). Bằng cách sử dụng các phần tử đàn hồi dạng dầm, thiết kế của gối đỡ đàn hồi có khả năng tạo ra biến dạng đàn hồi lớn trong khi vẫn duy trì được sự ổn định trong quá trình vận hành thực tế ở điều kiện tần số cao. Ngoài ra, thiết kế ổ đỡ được tối ưu hóa bằng phương pháp đáp ứng bề mặt (RSM) thông qua phần mềm ANSYS (được kết hợp với phân tích tĩnh trước đó bằng FEM) để đạt được kết cấu đàn hồi với khả năng biến dạng cao ở theo bậc tự do mong muốn. Các gối đỡ được tối ưu hóa và sau đó lắp ráp với bộ động cơ điện từ (VCA) để tạo ra một động cơ tuyến tính 1 bậc tự do không ma sát hoàn chỉnh, bộ VCA này được thiết kế để đáp ứng điều kiện về lực tối đa cần thiết cho một cặp cơ cấu đàn hồi với mối quan hệ tỉ lệ của lực và chuyển vị ~1. Một số đánh giá thực nghiệm sau đó được tiến hành để xác minh hoạt động thực tế của động cơ, ví dụ: hàm truyền có độ tuyến tính cao và sai số chuyển vị, dưới dòng điện DC đầu vào 0-5A. Kết quả thực nghiệm cho thấy rằng động cơ tịnh tiến được đề xuất có khả năng tạo ra chuyển động tịnh tiến chính xác cao và độ lặp lại cao ở mức  $\mu\text{m}$ . Hơn nữa, hành trình tối đa 6 mm của động cơ đủ lớn để tích hợp vào nhiều thiết bị cho các ứng dụng kỹ thuật yêu cầu độ chính xác cao và phạm vi hoạt động lớn như van điều khiển, bộ phận robot hoặc thậm chí truyền động trong không gian, v.v

**Từ khóa:** Động cơ tịnh tiến, gối đỡ đàn hồi, cơ cấu đàn hồi, tối ưu hóa, phương pháp bề mặt đáp ứng

**Trích dẫn bài báo này:** Nhân L H, Trường N H, Anh L T, Tuấn P M. **Mô hình động cơ tịnh tiến không ma sát với gối đỡ đàn hồi cho các ứng dụng trong cơ khí chính xác.** *Sci. Tech. Dev. J. - Eng. Tech.* 2024, 7(3):2380-2392.